Supplemental information to

Fine particles sampled at an urban background site and an industrialized coastal site in Northern France – Part 2: Comparison of offline and online analyses for carbonaceous aerosols

V. Crenn[1 ‡], A. Chakraborty[1], I. Fronval[1], D. Petitprez[2], V. Riffault[1 *]

[1] IMT Lille Douai, Univ. Lille, SAGE - Département Sciences de l'Atmosphère et Génie de l'Environnement, 59000 Lille, France

[2] PC2A, UMR CNRS-Lille1 8522, F-59655, Villeneuve d'Ascq, France

* Corresponding author: Véronique Riffault (veronique.riffault@imt-lille-douai.fr)

‡ Now at ADDAIR, F-78530 Buc, France

Materials and methods

1.1. Offline analyses

A low volume sampler (Partisol Speciation 2300 Model, Rupprecht & Patashnick Co.) allowed for the collection of $PM_{2.5}$ 24-hour samples on filters at a flow rate of 10 L min^{-1}. Quartz fiber filters (∅ = 47 mm, Tissuquartz 2500QAT-UP Pallflex, VWR) were pre-baked during 24h at 550°C in clean aluminum foil to remove any adsorbed organic material. Filters were collected every three days and after sampling, filters were wrapped individually in sealed Petri dishes and stored in a freezer at –20°C during transport and until analysis to prevent post-collection evaporation. All filter samples were analyzed in triplicates for each targeted chemical species and ambient levels were determined after subtracting the blank filter concentrations.

1.1.1. Polycyclic Aromatic Hydrocarbons (PAHs)

Filters were extracted by pressurized fluid extraction (ASE 200 Model, Dionex SA) in acetonitrile. Extract volumes were reduced to less than 1 mL under N_2 flow in a water bath held at 60°C (TurboVap® LV, Zymark) and then filtrated with a syringe membrane filter (Nylon, 0.2 µm pore size, Supelco Analytical) without further sample clean-up. PAHs were analyzed by High Performance Liquid Chromatography coupled to fluorescence detection (Alliance 2695/2475; Waters) at room temperature (20°C). The separation was performed on a Nucleosil C_{18} PAH column (250 mm × 2 mm, 5 µm; Macherey-Nagel) maintained at 30°C. A binary mobile phase consisting of (A) water and (B) acetonitrile (60:40, v/v) was used for the PAH elution at a constant flow rate of 0.3 mL min^{-1}. The elution program consisted of three linear gradients: first, from the initial proportions to 95% B (0 – 27.5 min); second, from 95 to 100% B (27.5 – 37.5 min) and third, from 100 to 40% B (37.5 – 45 min), followed by a 15-minute equilibration step in isocratic mode at 60% A (45 – 60 min). PAH calibrations were performed using an external standard method, with standard solutions ranging from 0.03 µg L^{-1} to 4 mg L^{-1} prepared from a PAH mixture containing 16 PAHs at various concentrations in acetonitrile (Ultra Scientific). The stability of the standards was measured over time with a new calibration performed when values exceeded ± 10% of the initial solution concentrations.

1.1.2. EC and OC measurements

$PM_{2.5}$ samples were analyzed for EC and OC concentrations by an EC/OC analyzer (Model 6.2, Sunset Laboratory Inc.) using a TOT method. A NIOSH-derived temperature program summarized in Table S1 was used, consisting in the introduction of a 1.5 cm^2 rectangular punch from filter subsamples in an oven heated stepwise, first in a non-oxidizing helium atmosphere leading to the gradual desorption of organic compounds as CO_2; second, after cooling down, the oven was heated up to 870°C under a He/O_2 atmosphere following increasing temperature steps then held at 870°C for the determination of EC. The transmittance or optical-attenuation (ATN)

was continuously monitored by a red light He-Ne laser (λ = 658 nm) through the quartz filter and used to define the EC/OC split-point and correct for pyrolyzed carbon (PC) produced during the He gas heating cycle. A 10 µL injection of an external standard of sucrose (Sigma Aldrich) at the concentration of 42.06 µgC cm^{-2} was performed every six samples as part of quality control. An uncertainty of the standard value higher than ±10 % was automatically rejected. An internal calibration using a CH_4 mixture was automatically injected at the end of every analysis in a fixed volume loop in order to compensate for the variability of the response of the FID. The measurement uncertainties were calculated combining statistical and systematic instrument uncertainties given by the manufacturer. Depending on the concentration levels, the calculated combined uncertainties were found to be 4 to 13% for OC and 6 to 21% for EC.

Table S1. Experimental parameters of the NIOSH-derived program

	Temperature (°C)	Hold time (s)	Carrier gas
OC1	310	105	He
OC2	475	85	He
OC3	615	50	He
OC4	870	25	He
	Oven off		He
EC1	550	65	He:O_2 (90%/10%)
EC2	625	48	He:O_2 (90%/10%)
EC3	700	40	He:O_2 (90%/10%)
EC4	775	35	He:O_2 (90%/10%)
EC5	850	25	He:O_2 (90%/10%)
EC6	870	25	He:O_2 (90%/10%)

1.2. Online analyses

Aerosols were sampled through a $PM_{2.5}$ cutoff inlet (2000-30EH, URG Cyclone) at a flow rate of 16.7 L min^{1} and transferred through stainless steel tubing using mass flow controllers to ensure isokinetic sampling.

1.2.1. Determination of BC by Aethalometer measurements

The operating principle of the Aethalometer consists in measuring the light attenuation (ATN) as follows:

$$\mathrm{ATN} = \ln\left(\frac{I_O}{I}\right) \quad \text{(S1)}$$

where I_0 is the intensity of the incoming light and I the remaining light intensity passing through the roll of the $PM_{2.5}$ loaded filter collected as a spot of area A = 0.5 cm^2. The relative uncertainty of the spot area was estimated to be ± 8% (Müller et al., 2011). I and I_0 parameters are linked by the Beer-Lambert's law defined as:

$$I = I_0 e^{-b_{abs} \cdot x} \tag{S2}$$

where b_{abs} is the absorption coefficient (m^{-1}) and x the thickness of the filter. Particle accumulation on filter during a time interval Δt changes the light attenuation defining the raw attenuation coefficient of the filtered aerosol particles b_{ATN} as:

$$b_{ATN,t} = \frac{(\mathrm{ATN}_t - \mathrm{ATN}_{t-1})}{\Delta t} \cdot \frac{A}{V} \tag{S3}$$

where V is the total sampled flow (3 L min^{-1}). When the spot reaches a certain density, the tape advances itself to collect aerosols on a new spot. Given the flow conditions and the averaging time (10 min), the Limit of Quantification (LOQ) for BC was calculated to be 167 ngC m^{-3}.

However sampling artifacts affect these filter-based measurements such as multiple scattering by the filter fibers which increases the optical path, scattering due to particles already collected on the filter and shadowing effect due to the accumulation of impacted particles (Arnott et al., 2005; Collaud Coen et al., 2010; Schmid et al., 2006; Virkkula et al., 2007; Weingartner et al., 2003). In this work, BC concentrations were corrected following the procedure proposed by Weingartner et al. (2003):

$$\begin{aligned} b_{abs,t} &= \frac{b_{ATN,t}}{C_{ref} \cdot R(\mathrm{ATN})_t} = \frac{b_{ATN,t}}{C_{ref} \cdot \left[\left(\frac{1}{f} - 1 \right) \cdot \frac{\ln(\mathrm{ATN}_t) - \ln(10)}{\ln(50) - \ln(10)} + 1 \right]} \\ &= \frac{b_{ATN,t}}{C_{ref} \cdot \left[\left(\frac{1}{m \cdot (1 - \omega_0) + 1} - 1 \right) \cdot \frac{\ln(\mathrm{ATN}_t) - \ln(10)}{\ln(50) - \ln(10)} + 1 \right]} \end{aligned} \tag{S4}$$

with ATN in percents and where C_{ref} is a constant (C_{ref} = 2.14), f is the filter loading correction parameter estimated as the slope of b_{ATN} vs. ATN curve, m is a constant (m = 0.87) and ω_0 defines the single scattering albedo. In the present work, average ω_0 values, estimated from the PHOTONS/AERONET network, were used for each campaign: 0.876 for Douai in summer, 0.960 and 0.878 for Grande-Synthe in summer and winter, respectively. Finally, BC mass concentrations were recalculated using:

$$m(BC)_{corrected,t} = \frac{b_{abs,t}}{SG_{BC}} \tag{S5}$$

where SG_{BC} = 14625 / λ (in m^2 g^{-1} with λ given in nm) corresponds to the spectral mass specific attenuation cross-section as provided by the manufacturer.

It is worth noting that at λ = 370 nm, BC_{UV} are expressed in terms of equivalent BC concentrations. BC_{UV} designates the aromatic organic material (e.g. some polycyclic aromatic hydrocarbons found in tobacco smoke, fresh diesel exhaust, and/or woodfire smoke) which absorbs in the UV spectral range.

1.2.2. HR-ToF-AMS measurements

Blanks were recorded every three days corresponding to ~30-minute data using a particle filter (Balston) according to the method described in the Jimenez Research Group Wiki (http://cires.colorado.edu/jimenez-group/wiki/index.php/Field_ToF-AMS_Operation). Standard calibration protocols used during the field campaigns, data saving and analysis can be found elsewhere, as well as the seasonal variations of the major families measured in non-refractory submicron particles for the four campaigns (Crenn et al., 2017).

The time-of-flight mass spectrometer can operate in the V-mode (higher sensitivity but low mass resolution) or in the W-mode (less sensitivity but higher mass resolution) alternately. In the V-mode, the Mass Spectra (MS) and the Particle Time-of-Flight modes (P-ToF) were each recorded during one minute to obtain the mass concentrations and the size distributions of major non-refractory species (organic matter - OM, nitrates, sulfates, ammonium or chlorides), respectively. Mass spectra acquired every 10 seconds were co-added and averaged over 2 minutes for each mode. HR-ToF-AMS measurements were used to derive (i) organic matter (OM_{AMS}) concentrations from V-mode measurements, (ii) the O/C elemental ratio which could be used to derive organic carbon concentrations (OC_{AMS}) from W-mode, and (iii) PAH concentrations in the V-mode.

. The shape and the porosity of the inverted-conical vaporizer can lead to particle bouncing, therefore to an incomplete detection of aerosol species (Matthew et al., 2008). This effect can be amplified by particle losses due to the lens transmission (Huffman et al., 2005). Collection efficiency (CE) may be influenced by several factors (Middlebrook et al., 2012) such as particle phase and water content in aerosol composition, high acidity, high fraction of nitrates (Crosier et al., 2007; Matthew et al., 2008) and the origins of emission sources. CE was corrected for PAH and organic species following the procedure given in Middlebrook et al. (2012) and its temporal profile can be found as a Supplementary Figure S1 in Crenn et al. (2017). Not drying the aerosol upstream the AMS inlet can eventually lead to some artifacts like the loss of submicron particles due to hygroscopic growth in the sampling line and an increase of the AMS collection efficiency (CE) for high RH attributed to reduced particle bouncing. An empirical correction in CE values for RH > 80% was suggested to account for particle bouncing from the vaporizer, due to the sticky nature of moist particles (Middlebrook et al., 2012). In summer, RH values at both sites were lower than 80% for 95% of the time; this means that summer campaigns were relatively artifact-free. In winter, however, ambient RH levels were > 80% at both sites about half of the time. In the absence of measurements of RH directly into the sampling line, one could only give an upper limit of the number of measurements impacted by the absence of correction for RH.

Considering both ambient RH and each corresponding composition-dependent CE (named "CE_dry" in Middlebrook et al.'s algorithm), the maximum proportion of data where a correction higher than 25% (that is to say within the AMS uncertainty limits) should be applied (if ambient RH was equal to sampling RH) would have been limited to 36% in DO and 30% in GS. Besides, at both sites, samples were drawn from the rooftop to the AMS via a stainless steel sampling line, kept at room temperature around 22°C. Due to winter temperatures of (1.9 ± 3.6)°C with a maximum at 10.4°C in DO, and (−1.0 ± 3.8)°C with a maximum at 8°C in GS, RH in the sampled flow entering the instrument would have been fairly lower than the ambient levels. Thus, the impact of RH may have been much lower than expected.

AMS data were analyzed using the standard AMS data analysis software packages (SQUIRREL v1.51H and PIKA v1.10H respectively) written in Igor Pro 6.22A (Wavemetrics). High resolution mass spectral data obtained in the W-mode allowed for the classification of ~400 integrated ions in 15 chemical families based on their chemical formulae, where each ion can only belong to a single chemical family. PAHs and organics were defined separately in the fragmentation table. Similarly to Dzepina et al. (2007), the AMS fragmentation table (Allan et al., 2004; Canagaratna et al., 2007) used to determine mass concentrations has been altered to take into account PAH masses with the same carbon number as the 10 PAHs measured from filter analysis. Thus besides the "PAH" class already defined by default (with masses ranging from C_{16} to C_{34}), a second "$PAH_{AMS\text{-}C16\text{-}C22}$" was created considering only PAHs with 16 to 22 carbons (m/z 202; 228; 252; 276; 278).

1.3. Data validation and comparison

The analytical methods used in this work have different time resolutions ranging from a few minutes to several days. In order to compare the ambient levels of pollutants, all concentrations were averaged over the instrument with the lowest time resolution. However, during some periods one or the other instrument were not operating (due to technical problems) thus measurement comparison was performed only when some criteria were met, which explains the different numbers of compared data. Data from the Aethalometer were validated only when they represented more than 80% of the corresponding sampling period of the filters.

Organic matter concentrations from AMS measurements ($[OM]_{AMS}$) could be converted to $[OC]_{AMS}$ using the OM_{AMS}/OC_{AMS} ratios determined by the instrument and averaged for each filter period in order to compare them with OC measurements from filter analyses ($[OC]_F$). When AMS data were missing in the High Resolution mode (several short periods during winter) or were invalidated (i.e AMS sampling time was less than 80% of the filter collection time), the average OM_{AMS}/OC_{AMS} ratio measured during the field campaign was used to replace the missing values. For summer datasets elemental analysis was not available due to the lower sensitivity of the High Resolution mode. However from the HR analysis of AMS V-mode data, OM/OC ratios for GS and DO summer were found to be 1.61 and 1.70, respectively. Therefore a constant value of 1.6 (also consistent with literature data – cf. (Turpin and Lim, 2001)) was preferred.

References

Ahmed, T., Dutkiewicz, V.A., Shareef, A., Tuncel, G., Tuncel, S., Husain, L., 2009. Measurement of black carbon (BC) by an optical method and a thermal-optical method: Intercomparison for four sites. Atmospheric Environment 43, 6305–6311. doi:10.1016/j.atmosenv.2009.09.031

Aiken, A.C., DeCarlo, P.F., Kroll, J.H., Worsnop, D.R., Huffman, J.A., Docherty, K.S., Ulbrich, I.M., Mohr, C., Kimmel, J.R., Sueper, D., Sun, Y., Zhang, Q., Trimborn, A., Northway, M., Ziemann, P.J., Canagaratna, M.R., Onasch, T.B., Alfarra, M.R., Prevot, A.S.H., Dommen, J., Duplissy, J., Metzger, A., Baltensperger, U., Jimenez, J.L., 2008. O/C and OM/OC Ratios of Primary, Secondary, and Ambient Organic Aerosols with High-Resolution Time-of-Flight Aerosol Mass Spectrometry. Environmental Science & Technology 42, 4478–4485. doi:10.1021/es703009q

Allan, J.D., Delia, A.E., Coe, H., Bower, K.N., Alfarra, M.R., Jimenez, J.L., Middlebrook, A.M., Drewnick, F., Onasch, T.B., Canagaratna, M.R., Jayne, J.T., Worsnop, D.R., 2004. A generalised method for the extraction of chemically resolved mass spectra from Aerodyne aerosol mass spectrometer data. Journal of Aerosol Science 35, 909–922. doi:10.1016/j.jaerosci.2004.02.007

Arnott, W.P., Hamasha, K., Moosmüller, H., Sheridan, P.J., Ogren, J.A., 2005. Towards Aerosol Light-Absorption Measurements with a 7-Wavelength Aethalometer: Evaluation with a Photoacoustic Instrument and 3-Wavelength Nephelometer. Aerosol Science and Technology 39, 17–29. doi:10.1080/027868290901972

Canagaratna, M.R., Jayne, J.T., Jimenez, J.L., Allan, J.D., Alfarra, M.R., Zhang, Q., Onasch, T.B., Drewnick, F., Coe, H., Middlebrook, A., Delia, A., Williams, L.R., Trimborn, A.M., Northway, M.J., DeCarlo, P.F., Kolb, C.E., Davidovits, P., Worsnop, D.R., 2007. Chemical and microphysical characterization of ambient aerosols with the aerodyne aerosol mass spectrometer. Mass Spectrometry Reviews 26, 185–222. doi:10.1002/mas.20115

Chan, T.W., Huang, L., Leaitch, W.R., Sharma, S., Brook, J.R., Slowik, J.G., Abbatt, J.P.D., Brickell, P.C., Liggio, J., Li, S.-M., others, 2010. Observations of OM/OC and specific attenuation coefficients (SAC) in ambient fine PM at a rural site in central Ontario, Canada. Atmospheric Chemistry and Physics 10, 2393–2411.

Collaud Coen, M., Weingartner, E., Apituley, A., Ceburnis, D., Fierz-Schmidhauser, R., Flentje, H., Henzing, J.S., Jennings, S.G., Moerman, M., Petzold, A., Schmid, O., Baltensperger, U., 2010. Minimizing light absorption measurement artifacts of the Aethalometer: evaluation of five correction algorithms. Atmospheric Measurement Techniques 3, 457–474. doi:10.5194/amt-3-457-2010

Crenn, V., Fronval, I., Petitprez, D., Riffault, V., 2017. Fine particles sampled at an urban background site and an industrialized coastal site in Northern France — Part 1: Seasonal variations and chemical characterization. Science of The Total Environment 578, 203–218. doi:10.1016/j.scitotenv.2015.11.165

Crosier, J., Jimenez, J.L., Allan, J.D., Bower, K.N., Williams, P.I., Alfarra, M.R., Canagaratna, M.R., Jayne, J.T., Worsnop, D.R., Coe, H., 2007. Technical Note: Description and Use of the New Jump Mass Spectrum Mode of Operation for the Aerodyne Quadrupole Aerosol Mass Spectrometers (Q-AMS). Aerosol Science and Technology 41, 865–872. doi:10.1080/02786820701501899

El Haddad, I., Marchand, N., Wortham, H., Piot, C., Besombes, J.-L., Cozic, J., Chauvel, C., Armengaud, A., Robin, D., Jaffrezo, J.-L., 2011. Primary sources of PM2.5 organic aerosol in an industrial Mediterranean city, Marseille. Atmospheric Chemistry and Physics 11, 2039–2058. doi:10.5194/acp-11-2039-2011

Favez, O., El Haddad, I., Piot, C., Boréave, A., Abidi, E., Marchand, N., Jaffrezo, J.-L., Besombes, J.-L., Personnaz, M.-B., Sciare, J., Wortham, H., George, C., D'Anna, B., 2010. Inter-comparison of source apportionment models for the estimation of wood burning aerosols during wintertime in an Alpine city (Grenoble, France). Atmospheric Chemistry and Physics 10, 5295–5314. doi:10.5194/acp-10-5295-2010

Huang, X.-F., He, L.-Y., Hu, M., Canagaratna, M.R., Kroll, J.H., Ng, N.L., Zhang, Y.-H., Lin, Y., Xue, L., Sun, T.-L., Liu, X.-G., Shao, M., Jayne, J.T., Worsnop, D.R., 2011. Characterization of submicron aerosols at a rural site in Pearl River Delta of China using an Aerodyne High-Resolution Aerosol Mass Spectrometer. Atmospheric Chemistry and Physics 11, 1865–1877. doi:10.5194/acp-11-1865-2011

Huffman, J.A., Jayne, J.T., Drewnick, F., Aiken, A.C., Onasch, T., Worsnop, D.R., Jimenez, J.L., 2005. Design, Modeling, Optimization, and Experimental Tests of a Particle Beam Width Probe for the Aerodyne Aerosol Mass Spectrometer. Aerosol Science and Technology 39, 1143–1163. doi:10.1080/02786820500423782

Husain, L., Dutkiewicz, V.A., Khan, A.J., Ghauri, B.M., 2007. Characterization of carbonaceous aerosols in urban air. Atmospheric Environment 41, 6872–6883. doi:10.1016/j.atmosenv.2007.04.037

Jeong, C.-H., Hopke, P.K., Kim, E., Lee, D.-W., 2004. The comparison between thermal-optical transmittance elemental carbon and Aethalometer black carbon measured at multiple monitoring sites. Atmospheric Environment 38, 5193–5204. doi:10.1016/j.atmosenv.2004.02.065

Matthew, B.M., Middlebrook, A.M., Onasch, T.B., 2008. Collection Efficiencies in an Aerodyne Aerosol Mass Spectrometer as a Function of Particle Phase for Laboratory Generated Aerosols. Aerosol Science and Technology 42, 884–898. doi:10.1080/02786820802356797

Middlebrook, A.M., Bahreini, R., Jimenez, J.L., Canagaratna, M.R., 2012. Evaluation of Composition-Dependent Collection Efficiencies for the Aerodyne Aerosol Mass Spectrometer using Field Data. Aerosol Science and Technology 46, 258–271. doi:10.1080/02786826.2011.620041

Müller, T., Henzing, J.S., de Leeuw, G., Wiedensohler, A., Alastuey, A., Angelov, H., Bizjak, M., Collaud Coen, M., Engström, J.E., Gruening, C., Hillamo, R., Hoffer, A., Imre, K., Ivanow, P., Jennings, G., Sun, J.Y., Kalivitis, N., Karlsson, H., Komppula, M., Laj, P., Li, S.-M., Lunder, C., Marinoni, A., Martins dos Santos, S., Moerman, M., Nowak, A., Ogren, J.A., Petzold, A., Pichon, J.M., Rodriquez, S., Sharma, S., Sheridan, P.J., Teinilä, K., Tuch, T., Viana, M., Virkkula, A., Weingartner, E., Wilhelm, R., Wang, Y.Q., 2011. Characterization and intercomparison of aerosol absorption photometers: result of two intercomparison workshops. Atmospheric Measurement Techniques 4, 245–268. doi:10.5194/amt-4-245-2011

Ram, K., Sarin, M.M., Tripathi, S.N., 2010. Inter-comparison of thermal and optical methods for determination of atmospheric black carbon and attenuation coefficient from an urban location in northern India. Atmospheric Research 97, 335–342. doi:10.1016/j.atmosres.2010.04.006

Schmid, O., Artaxo, P., Arnott, W.P., Chand, D., Gatti, L.V., Frank, G.P., Hoffer, A., Schnaiter, M., Andreae, T.W., 2006. Spectral light absorption by ambient aerosols influenced by biomass burning in the Amazon Basin. I: Comparison and field calibration of absorption measurement techniques. Atmospheric Chemistry and Physics 6, 3443–3462.

Stone, E.A., Lough, G.C., Schauer, J.J., Praveen, P.S., Corrigan, C.E., Ramanathan, V., 2007. Understanding the origin of black carbon in the atmospheric brown cloud over the Indian Ocean. J. Geophys. Res. 112, n/a-n/a. doi:10.1029/2006JD008118

Takegawa, N., Miyazaki, Y., Kondo, Y., Komazaki, Y., Miyakawa, T., Jimenez, J.L., Jayne, J.T., Worsnop, D.R., Allan, J.D., Weber, R.J., 2005. Characterization of an Aerodyne Aerosol Mass Spectrometer (AMS): Intercomparison with Other Aerosol Instruments. Aerosol Science and Technology 39, 760–770. doi:10.1080/02786820500243404

Turpin, B.J., Lim, H.-J., 2001. Species Contributions to PM2.5 Mass Concentrations: Revisiting Common Assumptions for Estimating Organic Mass. Aerosol Science and Technology 35, 602–610. doi:10.1080/02786820119445

Virkkula, A., Mäkelä, T., Hillamo, R., Yli-Tuomi, T., Hirsikko, A., Hämeri, K., Koponen, I.K., 2007. A Simple Procedure for Correcting Loading Effects of Aethalometer Data. Journal of the Air & Waste Management Association 57, 1214–1222. doi:10.3155/1047-3289.57.10.1214

Weingartner, E., Saathoff, H., Schnaiter, M., Streit, N., Bitnar, B., Baltensperger, U., 2003. Absorption of light by soot particles: determination of the absorption coefficient by means of aethalometers. Journal of Aerosol Science 34, 1445–1463. doi:10.1016/S0021-8502(03)00359-8

Zhang, Q., Canagaratna, M.R., Jayne, J.T., Worsnop, D.R., Jimenez, J.-L., 2005. Time- and size-resolved chemical composition of submicron particles in Pittsburgh: Implications for aerosol sources and processes. J. Geophys. Res. 110, n/a-n/a. doi:10.1029/2004JD004649

Table S2. OM_{AMS}/OC ratios measured in DO and GS during the winter field campaigns and at various sites around the world.

References	OC analytical method (PM size)	AMS version (NR-PM_1)	OM_{AMS}/OC	CE	Sampling site	Site	Seasons / Observations
This work	NIOSH-derived method ($PM_{2.5}$)	HR-ToF-AMS	1.63 [a] 1.88 [b] *	CE†	DO (FR)	urban	winter
(Takegawa et al., 2005)	NIOSH method ‡ (PM_1)	Q-AMS	1.61 [b] 1.79 [b]	0.5 0.5	Tokyo (JAP)	urban	spring summer
(Zhang et al., 2005)	IMPROVE method ($PM_{2.5}$)	Q-AMS	1.69 [b]	0.5	Pittsburgh (USA)	urban	autumn
(Aiken et al., 2008)	-	HR-ToF-AMS	1.71 [a]	0.5	Mexico (MEX)	urban	aircraft
(Favez et al., 2010)	EUSAAR 2 method ($PM_{2.5}$)	c-ToF-AMS	1.78 [b]	0.5	Grenoble (FR)	urban	winter
This work	NIOSH-derived method ($PM_{2.5}$)	HR-ToF-AMS	1.76 [a] 2.05 [b] *	CE†	GS (FR)	industrialized coastal	winter
(El Haddad et al., 2011)	NIOSH-method (PM_1)	c-ToF-AMS	1.67 [b]	0.5	Marseilles (FR)	urban / industrial	summer
(Chan et al., 2010)	"EnCan Total-900" method (PM_1)	c-ToF-AMS	1.58 [b] 2.08 [b]	0.5 0.5	Ontario (CAN)	rural	North wind South wind
(Huang et al., 2011)	-	HR-ToF-AMS	1.77 [a]	0.5	PRD (China) *	rural	winter (Asian monsoon)

[a] OM_{AMS}/OC_{AMS} ; [b] OM_{AMS}/OC_F; * the ratio was corrected to take into account the difference in size fraction (NR-PM_1/$PM_{2.5}$); † CE collection efficiency calculated following (Middlebrook et al., 2012); ‡ OC values were compared to those obtained with the IMPROVE protocol.

Table S3. Comparison between EC and BC concentrations (in µgC m^{-3}) and the corresponding linear regression from aerosol sampled at the two sampling sites and throughout the world.

Sampling site	Sampling period	EC		BC		BC/EC ratio	r^2	n	Reference
		[EC] (µgC m^{-3})	Analytical method	[BC] (µgC m^{-3})	Instrument				
Douai, FR (UB)	July–Aug. 2011	0.46 ± 0.18	NIOSH-derived method	0.32 ± 0.28	AE-21 Aethalometer	0.83 ± 0.05	0.97	10	This work[a]
Grande-Synthe, FR (IC)	May–June 2011	0.46 ± 10		0.29 ± 0.11		0.48 ± 0.10	0.81	7	
	Jan.–Feb. 2012	0.80 ± 0.39		0.67 ± 0.57		0.65 ± 0.14	0.64	15	
Kanpur, India (U)	Jan. 2007 – Feb. 2008	3.8	NIOSH method	4.5	Aethalometer	1.20	0.62	32	(Ram et al., 2010)[a]
Hanimaadhoo, Maldives (C)	Aug. 2004 – Jan. 2005	1.11 ± 0.09†	ACE-Asia method	n/a	Aethalometer	n/a	0.968	n/a	(Stone et al., 2007))[b]
Gan, Maldives (C)	Sept.–Nov. 2004	0.254 ± 0.055†		n/a					
Rochester, USA (T)	June 2002	0.4	NIOSH method	0.9	AE-20 Aethalometer	3.3	0.84	60	(Jeong et al., 2004))[c]
Philadelphia, USA (T)	July–Aug. 2002	0.4		0.9		2.7	0.60	281	
Lahore, Pakistan (U)	Nov. 2005 – Jan. 2006	17.4	NIOSH-derived method	21.7 ± 6.6	AE-21 Aethalometer	1.25	0.71	81	(Husain et al., 2007)[c]
Albany, USA (U)	May–June 2002 and Oct.–Dec. 2003	0.560	NIOSH method	0.550	OT-21 Optical Transmissiometer	1.02	0.88†	35	(Ahmed et al., 2009)[c]
Antalya, Turkey (C)	Sept.–Dec. 1993	0.590		0.640		1.02	0.50	41	
Whiteface Mountain, USA (R)	1996 and Jan.–Feb. 2002	0.215		0.215		0.92	0.58	206	
Mayville, USA (R)	Aug. 1990, 1998, 2002 and July 2002	0.520		0.435		0.75	0.44	192	

UB: urban background; IC: industrialized coastal; U: urban; C: coastal; T: traffic; R: remote/rural; RB: regional background; n/a: no data available; † after exclusion of two outliers. BC concentrations were corrected from reported procedures proposed by: [a] Weingartner et al., 2003; [b] Arnott et al., 2005; [c] BC correction not mentioned.

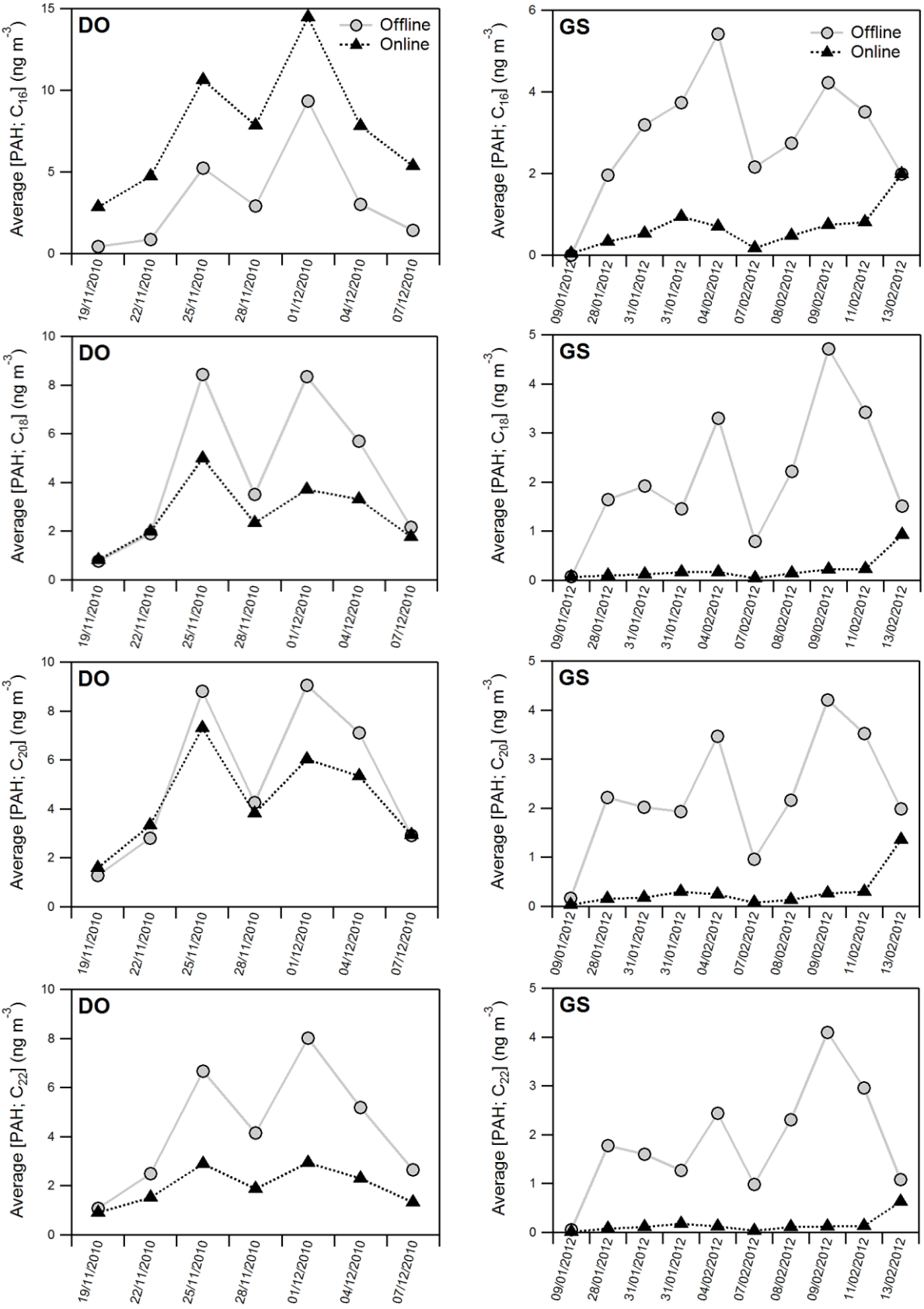

Figure S1. Time series from the winter campaigns performed in (left) DO and (right) GS of the (from top to bottom) C_{16}, C_{18}, C_{20} and C_{22} PAH concentrations measured by online AMS (black triangles) and from offline analysis of daily $PM_{2.5}$ filter samples collected in winter (grey circles). PAH_{AMS} concentrations were averaged over the same sampling time as filters, considering a constant collection efficiency of 0.5 and a Relative Ionization Efficiency (RIE) of 1.4, similar to the organics.

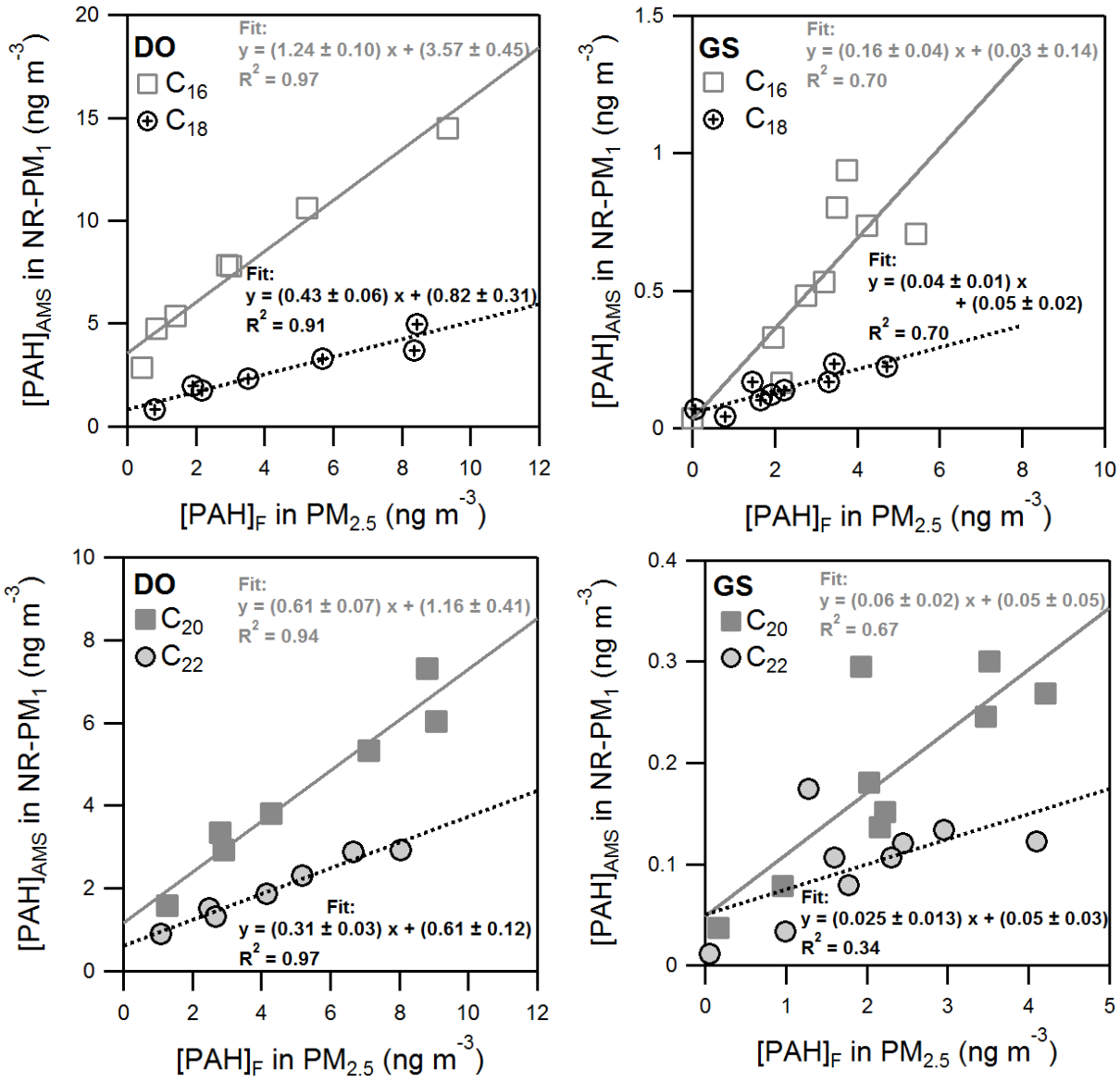

Figure S2: Scatter plots of PAH measurements performed in (left) DO and (right) GS comparing (top) C_{16} (open squares), C_{18} (open circles), (bottom) C_{20} (solid squares) and C_{22} (solid circles) concentrations between both methods. The lines are the corresponding linear regression fits through the data (coefficients are given with a 1σ statistical uncertainty). For GS, one outlier was excluded.

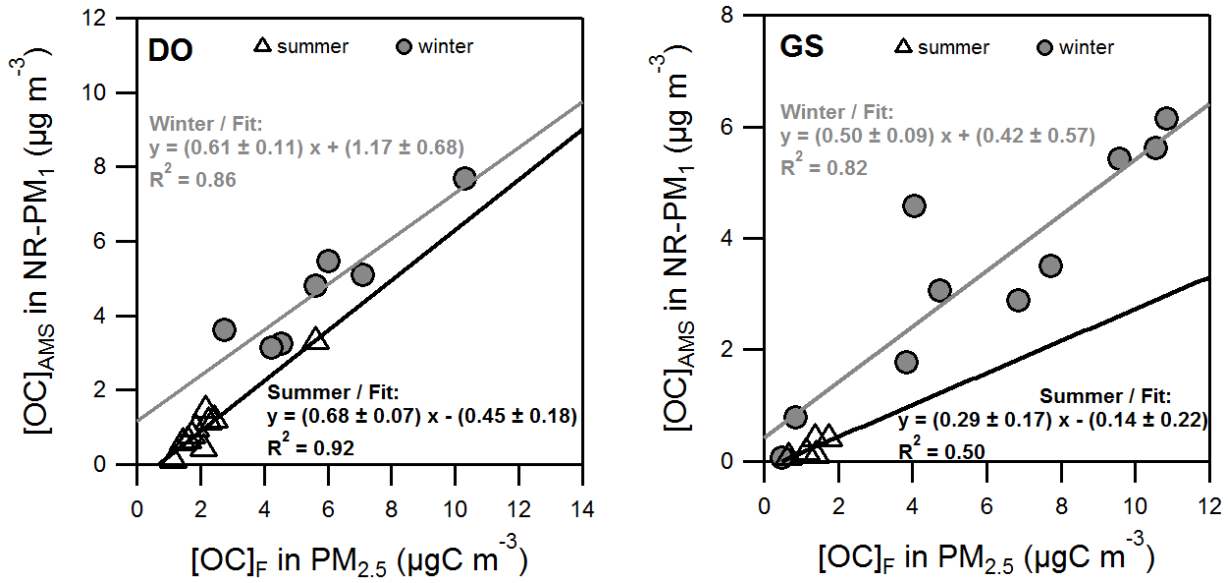

Figure S3. Comparison of [OC] measured by the AMS vs. measured by the EC/OC analyzer in (left) DO and (right) GS during the winter (solid circles) and summer (open triangles) sampling periods. The lines are the corresponding linear regression fits through the data (coefficients are given with a 1σ statistical uncertainty).

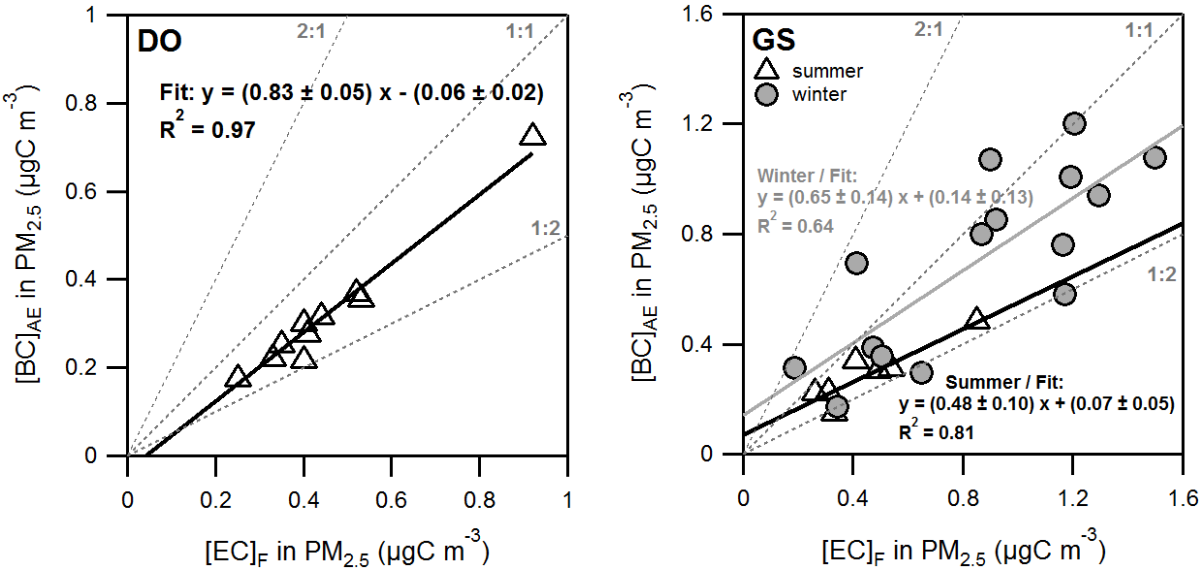

Figure S4. Scatter plots of $[BC]_{AE}$ vs.$[EC]_F$ measured in (left) DO in summer (open triangles; n = 10) and (right) GS during the winter (solid circles; n = 15) and summer (open triangles; n = 7) sampling periods. The solid lines are the corresponding linear regression fits through the data (coefficients are given with a 1σ statistical uncertainty).